Effects of Protein Source on Liposome Uptake by Cells

Yang, Keni; Reker-Smit, Catharina; Stuart, Marc C A; Salvati, Anna

Published in:
Advanced healthcare materials

DOI:
10.1002/adhm.202100370

Publication date:
2021

ADVANCED HEALTHCARE MATERIALS
www.advhealthmat.de

Effects of Protein Source on Liposome Uptake by Cells: Corona Composition and Impact of the Excess Free Proteins

*Keni Yang, Catharina Reker-Smit, Marc C. A. Stuart, and Anna Salvati**

Corona formation in biological fluids strongly affects nanomedicine interactions with cells. However, relatively less is known on additional effects from the free proteins in solution. Within this context, this study aims to gain a better understanding of nanomaterial–cell interactions in different biological fluids and, more specifically, to disentangle effects due to corona composition and those from the free proteins in solution. To this aim, the uptake of liposomes in medium with bovine and human serum are compared. Uptake efficiency in the two media differs strongly, as also corona composition. However, in contrast with similar studies on other nanomaterials, despite the very different corona, when the two corona-coated liposomes are exposed to cells in serum free medium, their uptake is comparable. Thus, in this case, the observed differences in uptake depend primarily on the presence and source of the free proteins. Similar results are obtained when testing the liposomes on different human cells, as well as in murine cells and in the presence of murine serum. Overall, these results show that the protein source affects nanomedicine uptake not only due to effects on corona composition, but also due to the presence and composition of the free proteins in solution.

1. Introduction

The application of nanotechnology for medical purposes has attracted great interest in the past few decades, since nanosized materials have been proposed as a delivery platform for drugs, genes, and therapies to treat and diagnose various diseases.[1–4] Benefiting from their nanoscale size and surface properties, nanomaterials can be designed to increase the payload of drugs and accumulate efficiently in diseased cells and tissue via the so-called enhanced permeability and retention effect for "passive targeting"[5,6] or via grafted ligands on the material surface for "active targeting."[7–10]

However, the clinical translation of nanomedicine remains highly challenging. Even if thousands of papers on nanomedicine are published per year, relatively few new nanoformulations have been approved for clinical use.[11] One of the main obstacles remains the (often) still limited understanding of the interactions of nanomaterials with cells, tissues, and the biological environments in which they are applied.[12,13] Generally, in vitro experiments to evaluate nanomedicine efficiency and toxicity are performed with human cell lines cultured in medium supplemented with fetal bovine serum (FBS) (FBS is a universal animal serum supplement for cells and tissue culture media[14]). However, once introduced into a biological environment, nanomaterials are rapidly covered with plenty of proteins and other biomolecules, forming a layer known as "protein corona".[15,16] The protein corona confers nanomaterials new biological properties by altering their size distribution, surface charge, aggregation behavior, interfacial character, as well as by decorating the nanomaterial surface with specific proteins and epitopes, capable to interact with and be recognized by specific cell receptors.[17–24] This, in turn, can affect the following nanoparticle interactions with cells or tissues, as well as their final fate in vivo.[21,25,26] As a consequence of this, different outcomes are expected when nanomaterials are exposed to different biological fluids (for instance serum versus lung fluids, depending on the administration or exposure route).[27,28] Furthermore, it has been shown that even when considering the same biological fluid, differences in the protein source affect corona formation as well as the subsequent nanomaterial interactions with cells. For instance, Solorio-Rodríguez et al. reported differences in protein-corona composition on functionalized SiO_2 nanocarriers after incubation with human plasma or mouse plasma.[29] Similar studies by Müller et al. revealed discrepancies in aggregation behavior and corona composition of nanoparticles when recovered from human, mouse, rabbit, or

Dr. K. Yang[+], C. Reker-Smit, Prof. A. Salvati
Department of Nanomedicine and Drug Targeting
Groningen Research Institute of Pharmacy
University of Groningen
A. Deusinglaan 1, Groningen 9713 AV, The Netherlands
E-mail: k.yang@rug.nl; a.salvati@rug.nl
Dr. M. C. A. Stuart
Groningen Biomolecular Sciences and Biotechnology Institute
University of Groningen
Nijenborgh 74, Groningen 9747 AG, The Netherlands

The ORCID identification number(s) for the author(s) of this article can be found under https://doi.org/10.1002/adhm.202100370

[+]Present address: Key Laboratory for Nano-Bio Interface Research, Division of Nanobiomedicine, Suzhou Institute of Nano-Tech and Nano-Bionics, Chinese Academy of Sciences, Suzhou 215123, China

DOI: 10.1002/adhm.202100370

sheep plasma.[30] Schöttler et al. also showed different uptake by cells for polystyrene nanoparticles incubated in FBS, human serum (HS), and human plasma.[31] These studies show that nanomedicines added to cells in FBS medium in in vitro studies, or exposed to serum of a different species once tested in vivo, including human plasma when they finally reach clinical trials, are likely to be covered by different protein coronas.[32] This suggests that the biological responses and therapeutic outcomes observed in vitro may not be directly translated to clinical use.[33–34]

While similar effects of the protein source on corona composition have been reported and—at least in part—characterized, much less is known on potential effects related to the presence of excess free proteins in solution. Previous studies showed that the addition of human serum in the medium (as opposed to FBS) usually decreases nanoparticle uptake and a lower uptake is observed when serum concentration is increased.[19,23,35] Similarly, Schöttler et al. reported that the uptake of polystyrene nanoparticles in medium with FBS was high, while when added to cells in human serum it was almost not detectable.[31] However, an explicit distinction of the effects of the protein source on corona composition and due to the presence of free proteins in solution has not been performed as yet.

To this aim, in this work, liposomes composed of 1,2-dioleoyl-sn-glycero-3-phospho-(1′-rac-glycerol) (DOPG) and DC-cholesterol (DOPG-DC liposomes) were used as a nanomedicine model. The cellular uptake of DOPG-DC liposome exposed to cells in FBS and HS was compared, as also their protein corona composition. Thus, corona-coated liposomes were isolated from both media and added to cells in serum-free conditions or after addition to media supplemented to either FBS or HS. This has allowed us to differentiate effects of the protein source on corona composition from those due to the excess free proteins in solution.

2. Results and Discussion

2.1. Liposome Preparation and Characterization

Liposomes were chosen as a nanomedicine model because they constitute one of the most clinically established nanobased drug delivery systems. Since the approval in 1995 of Doxil, pegylated liposomal doxorubicin, several liposomal formulations have been approved for clinical use, making liposomes the most represented formulation among the approved nanomedicines.[36,37] Thus, DOPG-DC liposomes composed of the negatively charged DOPG lipid and the positively charged DC-cholesterol (see chemical structures in **Figure 1**A) were prepared by thin lipid film hydration followed by repeated freeze–thaw cycles and extrusion.[38] The hydrophilic dye sulforhodamine B (SRB) was incorporated in the inner aqueous volume of the liposomes in order to obtain fluorescently labeled liposomes, thus to quantify cellular uptake and visualize their intracellular location (Figure 1B). The size distribution by dynamic light scattering (DLS) and zeta potential of the liposomes were measured after extrusion and dispersion in different media (Figure 1C–F), including phosphate-buffered saline (PBS) and the cell culture medium (MEM) supplemented with either 10% FBS (fbsMEM), corresponding to roughly 4 mg mL^{-1} proteins, or the same concentration of HS (hsMEM). Liposomes dispersed in PBS had a negative zeta potential around −33 mV and an average diameter of around 139 nm, consistent with the size expected after extrusion through a 100 nm filter. The low polydispersity index (PDI) confirmed that highly monodispersed liposomes could be obtained by this method. When introduced into fbsMEM or hsMEM, the liposome size slightly increased to around 170 nm and the zeta potential shifted toward neutrality, as expected following serum proteins adsorption on the liposome surface and corona formation. The DOPG-DC liposomes remained stable in cell culture condition (5% CO_2 at 37 °C) for up to 24 h (Figure 1D,E and Table S1, Supporting Information) (in some cases a small peak at around 10 µm was also detected, likely due to the presence of few protein aggregates, to which DLS is highly sensitive).

2.2. Internalization Studies

In order to compare liposome–cell interactions in media supplemented with serum proteins from a different source, the uptake of 50 µg mL^{-1} DOPG-DC liposomes in 4 mg mL^{-1} fbsMEM or hsMEM (roughly corresponding to a protein to lipid ratio of 80:1) was measured by flow cytometry. Human epithelial cervical cancer HeLa cells were used for this purpose, as a common model for similar studies and cell fluorescence was measured by flow cytometry over time during continuous exposure. The uptake kinetics showed that the liposomes exposed to cells in fbsMEM had much higher uptake compared to those in hsMEM (**Figure 2**A) (We note a peculiar decrease in average cell fluorescence after the first hours of exposure, particularly in hsMEM, as previously observed for comparable DOPG liposomes,[39] which is the object of ongoing studies). In the presence of the metabolic inhibitor sodium azide to deplete the cell energy, liposome uptake dropped substantially both in fbsMEM and hsMEM (Figure 2B,C). This indicated that in both media liposomes were taken up as intact nanoparticles following energy-dependent mechanisms (instead of passive mechanisms of direct fusion with the cell membrane).

Next, confocal fluorescence imaging was used to confirm liposome internalization and determine their final intracellular location. As shown in Figure 2D,E, after 2 h incubation with cells, for the liposomes dispersed in fbsMEM a clear intracellular signal was detected, and most liposomes were colocalized with intracellular vesicles stained by LysoTracker, likely the lysosomes (Figure 2D). However, in agreement with the lower uptake observed by flow cytometry (Figure 2A), liposomes dispersed in hsMEM were barely detected inside cells when using the same imaging settings (Figure 2E). Only when the gain of the detector was increased, liposome uptake was confirmed also in hsMEM, as well as the colocalization with LysoTracker (Figure 2F).

The strong difference observed in cellular uptake for liposome dispersed in FBS and HS is in agreement with previous results for other nanoparticles in similar conditions.[31,35] We then asked whether the effect was triggered by potential differences in corona composition or by additional effects due to the presence of free serum proteins of different source in the media.

2.3. Isolation and Characterization of Corona-Coated Liposomes

In order to explain the different uptake efficiency in fbsMEM and hsMEM (Figure 2), as a first step the corona formed on the

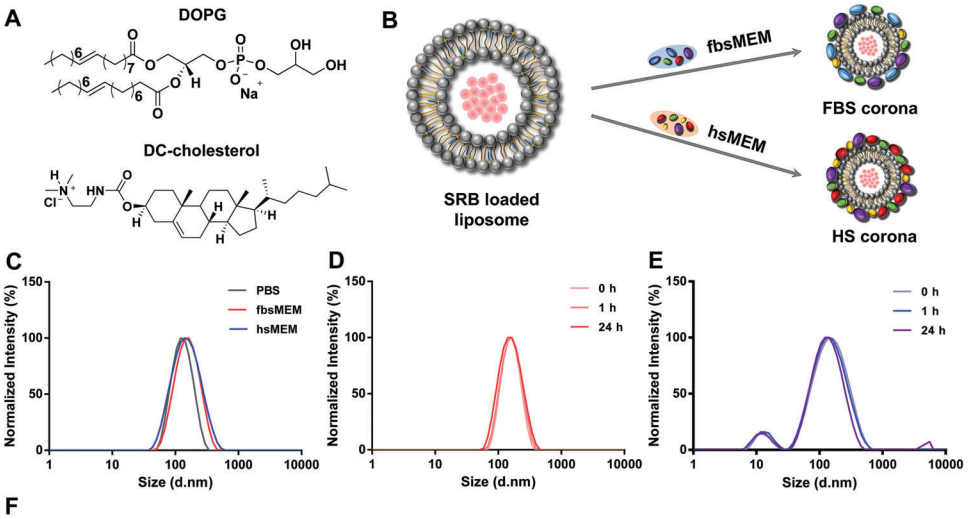

F

	PBS	fbsMEM	hsMEM
Diameter (z-average, nm)	117 ± 0.2	-	-
PDI	0.16 ± 0.02	-	-
Diameter (nm)	-	163 ± 3	175 ± 9
Zeta potential (mV)	-33 ± 3	-10 ± 3	-7 ± 1

Figure 1. Characterization of DOPG-DC liposomes. A) Chemical structures of DOPG lipid and DC-cholesterol. B) Schematic diagram of sulforhodamine B (SRB) loaded liposomes and FBS and HS corona formation on liposomes introduced in cell culture medium (MEM) supplemented with 4 mg mL^{-1} FBS (fbsMEM) or human serum (hsMEM). C–F) 50 µg mL^{-1} liposomes were dispersed in PBS, fbsMEM, or hsMEM and characterized by dynamic light scattering (DLS) and zeta potential measurements. For each sample, three measurements were performed and the size distribution of a representative measurement is shown. C) Size distributions by intensity (diameter, nm) of DOPG-DC liposomes in different media as obtained by DLS. The results showed that liposomes were monodispersed and remained stable when dispersed in different media. Stability of DOPG-DC liposomes in D) fbsMEM or E) hsMEM in cell culture conditions (37 °C, 5% CO_2). The size distribution of the liposome dispersions in different media were characterized by DLS at 0, 1, and 24 h after dispersion. The results showed that the liposomes remained stable in these conditions for up to 24 h. For the liposomes in hsMEM, in some measurements peaks around 10 and 10 000 nm were also visible, likely due to the presence of excess free proteins in solution. F) Diameter and zeta potential of DOPG-DC liposomes in different media. For the samples in PBS, the Z-average and polydispersity index (PDI) obtained from cumulant fitting of the data are shown, while for the liposomes dispersed in fbsMEM and hsMEM, where multiple populations are present, the average hydrodynamic diameter determined from CONTIN analysis is indicated. The results are the average and standard deviation of three measurements on the same sample.

liposomes in the presence of serum of different source was characterized. Despite several papers have reported already differences in corona composition when magnetic nanoparticles,[32] silica,[29] or polystyrene nanoparticles[31] isolated after dispersion in serum or plasma of different source, relatively few similar studies have been performed with liposomes before.[40] Liposomes have a lower density compared to the nanoparticles mentioned above, thus centrifugation may not be appropriate for corona isolation, since sedimentation is more difficult and using higher centrifugal forces could result in strong agglomeration which may affect corona composition.[41,42] Therefore, we isolated corona-coated liposomes from fbsMEM and hsMEM by size exclusion chromatography (SEC). In a previous study, where this method was carefully optimized, we showed that corona-coated liposomes could be isolated with excellent reproducibility.[39]

Given that the corona composition changes with the ratio between protein content and nanomaterial surface area,[43] in order to form the same corona as in the cell uptake studies, corona-coated liposomes were recovered from FBS (FBS corona) by SEC after incubation of FBS and DOPG-DC liposomes at a protein to lipid ratio of 80:1 w/w for 1 h (Figure S1, Supporting Information). For samples in HS (HS corona), we first used SEC to deplete the human serum of larger particles (Figure S1C, Supporting Information) and collected the cleaned HS for the preparation of HS corona. We previously showed that full HS contains particles of sizes comparable to the liposomes, which could contaminate liposome-corona complex during SEC isolation and thus confuse corona characterization.[39] Similar observations were also reported in literature.[44,45] Even though this procedure will slightly affect the final corona composition in HS, this method was preferred to ensure that no residual free proteins misinterpreted as corona proteins could be included. Then, liposomes were dispersed in the cleaned HS using the same conditions (protein to lipid ratio 80:1 w/w for 1 h) and the corona-coated liposomes were isolated by SEC (Figure S1D,E, Supporting Information). Fluorescence measurements of the eluted fractions (Figure S1B,E, Supporting Information) showed that most SRB eluted together with the liposome fractions (fraction 7–11), thus SRB remained encapsulated in the liposomes after incubation with serum, confirming liposomes stability.

DLS measurements before and after corona isolation showed that the hydrodynamic diameter slightly increased from 136 nm in PBS to 161 and 153 nm, respectively, for the FBS and HS corona, while the PDI remained low. This indicated successful

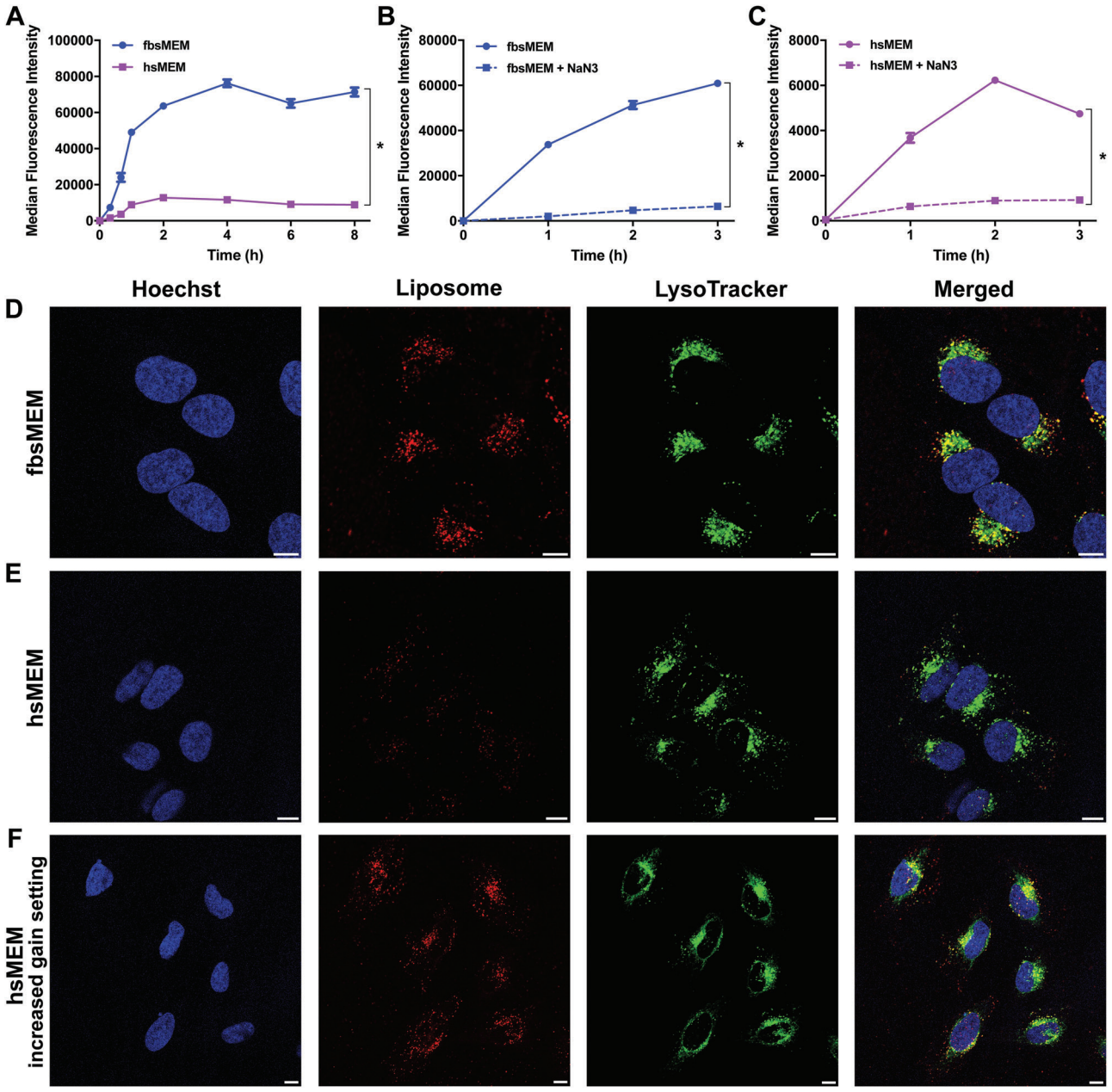

Figure 2. Internalization studies of the DOPG-DC liposomes in fbsMEM and hsMEM. A) Uptake kinetics by flow cytometry of DOPG-DC liposomes (50 μg mL^{-1}) added to HeLa cells in fbsMEM and hsMEM. The results showed that the uptake of liposomes was much higher in fbsMEM than in hsMEM. Uptake kinetics of liposomes in B) fbsMEM or C) hsMEM in the presence of sodium azide (NaN_3). 50 μg mL^{-1} liposomes in fbsMEM or hsMEM were added to cells in standard conditions or in the presence of 5 mg mL^{-1} sodium azide to deplete cell energy (see the Experimental Section for details). The strong decrease of uptake in the presence of sodium azide indicated that in both media liposomes were internalized by cells following energy-dependent pathways. The results in panels (A)–(C) are the average and standard deviation over duplicate samples of the median cell fluorescence intensity obtained by flow cytometry in a representative experiment (error bars are included in all graphs, but in some cases are not visible because very small). All experiments were repeated at least two times to confirm reproducibility. D–F) Confocal fluorescence images of HeLa cells exposed for 2 h to 50 μg mL^{-1} liposomes in D) fbsMEM or E,F) hsMEM. Blue: Hoechst stained nuclei. Red: liposomes. Green: LysoTracker Deep Red. Scale bar: 10 μm. The results confirmed that liposomes were internalized by cells and trafficked in LysoTracker stained compartments, likely the lysosomes. E) In agreement with flow cytometry, lower uptake was observed in hsMEM; F) however, also in this case uptake was confirmed when images were taken with increased gain settings. A Friedman test with time as blocking factor was performed in (A)–(C) when comparing uptake kinetics in two conditions. $p < 0.05$ was considered significant (indicated with *).

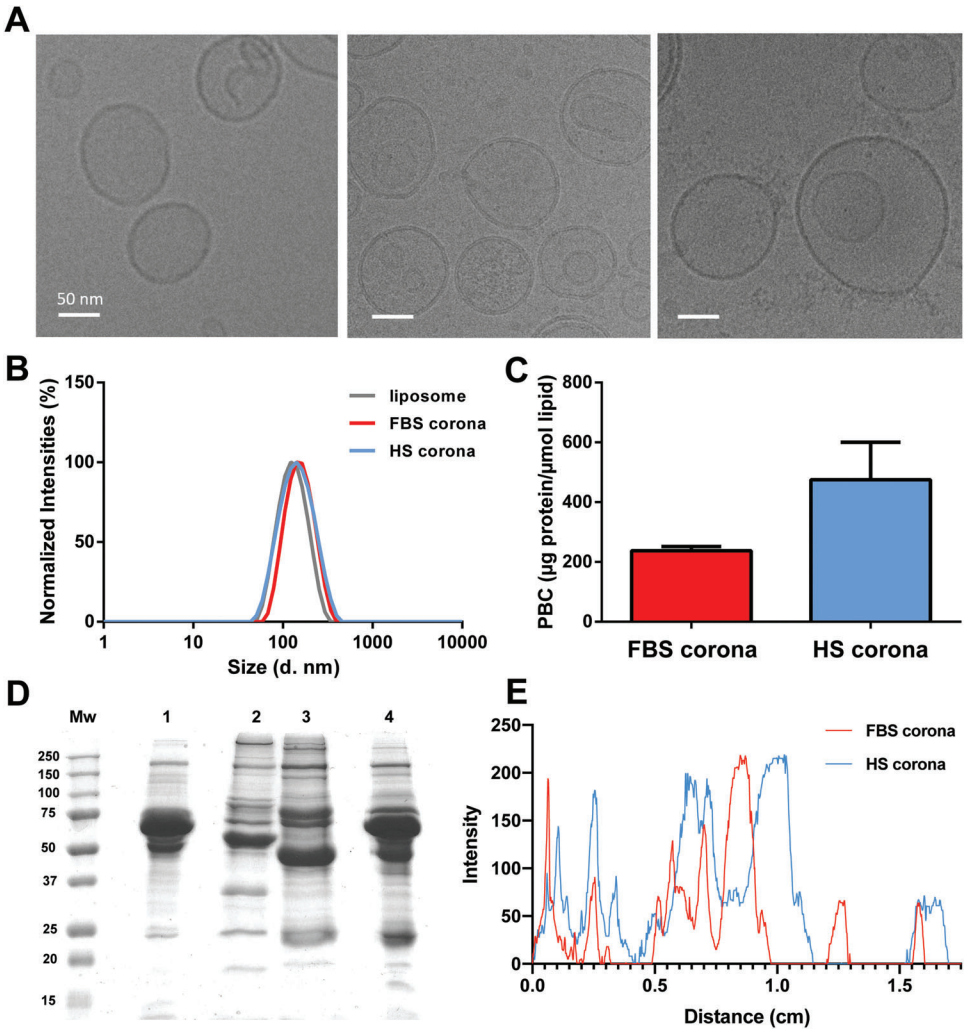

Figure 3. Characterization of DOPG-DC liposome corona in FBS or cleaned HS. A) Cryo-EM images of DOPG-DC liposomes dispersed in PBS (left panel) and corona-coated liposomes isolated from FBS and HS (middle and right panels, respectively). Scale bar: 50 nm. B) Size distribution by intensity obtained by DLS of 50 µg mL^{-1} liposomes dispersed in PBS and corona-coated liposomes recovered from FBS (FBS corona) or cleaned HS (HS corona). A representative size distribution out of three measurements is shown (the corresponding average and standard deviation are given in Table S1, Supporting Information). C) Comparison of the protein binding capacity (PBC) of liposomes dispersed in FBS or cleaned HS. The PBC value was calculated as the amount of corona proteins (µg) from FBS or cleaned HS per micromole lipid (see the Experimental Section for details). The data are the mean and standard deviation of the results obtained on two independent liposome batches and corona isolations. A Mann–Whitney test (two-tailed) was performed and indicated that the difference between the two groups was not statistically significant ($p < 0.05$ was considered significant). D) SDS-PAGE image of the corona proteins recovered on DOPG-DC liposomes in FBS (lane 2) or cleaned HS (lane 3). The same amount of liposomes were loaded (corresponding to 0.05 µmol lipid). Additionally, 20 µg of FBS (lane 1) or cleaned HS (lane 4) were loaded as controls. Lane 1: 20 µg FBS; lanes 2 and 3: corona-coated liposomes isolated from FBS (FBS corona) or from cleaned HS (HS corona), respectively; lane 4, 20 µg cleaned HS. A representative SDS-PAGE image is shown out of three repeated experiments with independent liposome batches and corona isolations. E) Intensity profiles of all bands of FBS and HS corona in the SDS-PAGE image shown in Figure 3D. A,B) The results showed that SEC allowed to isolate homogenous dispersions of corona-coated liposomes. C) The PBC and D,E) the corona composition were different in the two media.

isolation of an homogenous dispersion of corona-coated liposomes, as also confirmed by cryo-EM (cryogenic electron microscopy) imaging (**Figure 3**A,B and Table S1, Supporting Information). Next, in order to determine potential differences in the two media, the protein binding capacity (PBC) expressed as the amount of corona proteins (µg of protein) per micromole of lipid was determined (see the Experimental Section for details), and gel electrophoresis (sodium dodecyl sulfate-polyacrylamide gel electrophoresis (SDS-PAGE)) was used to separate the isolated corona proteins (Figure 3C,D and additional controls in Figure S2, Supporting Information, to exclude interference of the liposomes with protein quantification). The results suggested that the DOPG-DC liposome isolated from cleaned HS absorbed a higher amount of proteins compared with the one recovered from FBS (Figure 3C). Although this difference was not statistically significant, SDS-PAGE results also showed bands of higher intensity for the HS corona than the FBS corona (Figure 3D, lines 3 and 2, respectively). Interestingly, even though the FBS and cleaned HS alone (Figure 3D, lines 1 and 4, respectively) had similar band patterns, the band pattern detected in the FBS and HS

coronas differed strongly, as also confirmed by quantification of the intensities of all bands (Figure 3E). These results indicated that not only the liposomes absorbed different amounts of proteins in the two media, but, in agreement with previous works with other nanoparticle types, they also formed different protein coronas when introduced in serum of different source.[29,31,46]

Label-free liquid chromatography tandem mass spectrometry (LC-MS/MS) was used to further compare the protein composition of the corona from the two media as well as of FBS and cleaned HS (Tables S2 and S3 and Figure S3, Supporting Information and Supplementary File with the complete mass spectrometry results). As also visible by SDS-PAGE (Figure 3D), albumin, with a molecular weight around 66 kDa, was the most abundant protein in both sera, where it accounted for more than 50% of total protein composition (Table S2, Supporting Information). Interestingly, the human serum contained more immunoglobulins, apolipoproteins and acute phase proteins (Figure S3C, Supporting Information) and also more proteins with positive charge in physiological conditions (isoelectric point > 7.4) (Figure S3B, Supporting Information), while immunoglobulins were barely detected in FBS, a difference which was previously reported.[34] When comparing the corona formed on the liposomes in the two types of serum, 76 of the identified proteins were common to both coronas and around 200 unique proteins were identified in each sample (Figure S3G, Supporting Information). The FBS corona included around 70% apolipoproteins and 10% coagulation proteins, while the HS corona was composed of around 40% apolipoproteins, 30% immunoglobulins and 10% acute phase proteins (Figure S3F, Supporting Information). The strong difference in the amount of immunoglobulins detected in the FBS corona is likely to result from the much lower amount of immunoglobulins contained in FBS. The FBS corona also contained higher amounts of proteins with molecular weight between 20–40 kDa (around 50%), while ≈ 40% of the HS corona proteins had a molecular weight below 20 kDa (Figure S3D, Supporting Information). Additionally, although proteins with isoelectric point between 5 and 6 were present in both corona samples, the most negative proteins (isoelectric point < 5) were strongly enriched in the FBS corona, where they constituted 25% of the total proteins recovered, as opposed to only 5% in the HS corona. Vice versa, positively charged proteins (isoelectric point > 7.4) were more abundant in the HS corona (26% and 6% in HS and FBS corona, respectively) (Figure S3E, Supporting Information).

Taken together, the LC-MS/MS results confirmed that the liposomes formed a very different corona not only in relation to the amount of adsorbed proteins but also their type, charge, and molecular weight. These differences likely result from the different composition of bovine and human serum.

2.4. Effect of Protein Source on Uptake Behavior

In order to understand if the observed differences in corona composition played a role in the different cellular uptake behavior, we excluded the excess free proteins in the medium and exposed HeLa cells to the isolated FBS and HS corona-coated liposomes in serum free conditions (sfMEM) (**Figure 4**A,B). A schematic diagram of the experimental process is shown in Figure 4A. Interestingly, this allowed us to determine that despite the very different corona, the two corona-coated DOPG-DC liposomes showed very similar uptake efficiency (Figure 4B, solid and dashed gray lines). We then reintroduced the FBS and HS corona-coated liposomes in either fbsMEM or hsMEM and compared their uptake levels in the same medium. Once reintroduced in hsMEM, the two corona-coated liposomes showed comparable uptake (Figure 4B, solid and dashed purple lines). This also allowed us to exclude that the similar uptake observed for the two corona-coated liposomes was due to changes in cell activity because of serum deprivation. Comparable uptake was observed also for the two corona-coated liposomes re-introduced in fbsMEM (Figure 4B, solid and dashed blue lines). Interestingly, in fbsMEM uptake levels were much higher than in sfMEM. This may be due to adsorption of some additional corona proteins from fbsMEM promoting cell uptake. Alternatively, the higher uptake may be due to competition of free proteins in fbsMEM for cell receptors and displacement of the corona-coated liposomes to a different receptor with higher uptake efficiency. Identifying the receptors involved in uptake in all the different conditions would be important to clarify this observation.

In order to determine if the re-introduction of the corona-coated liposomes in fbsMEM or hsMEM led to formation of a different corona, the corona-coated liposomes were isolated again by SEC, and corona proteins identified by SDS-PAGE (Figure 4C). When the FBS corona was introduced in human serum (line 3), some of the bands of the FBS corona (line 1) reduced their intensity and new bands which were present in the HS corona (line 4) appeared. Similar results were observed for the HS corona when reintroduced in FBS (line 5). This was further confirmed by quantification of the intensity of all bands (Figure 4D). Thus, as expected, the corona composition changed when the corona-coated liposomes were reintroduced in a serum of different source and composition. Nevertheless, clear differences in the FBS and HS coronas remained still visible, even once reintroduced in the same serum (Figure 4C,D, lanes 2 and 5 for fbsMEM and 3 and 6 for hsMEM).

We then performed comparable experiments for silica nanoparticles in FBS and HS. In this case, after isolation of corona-coated silica, uptake was much higher for the FBS corona than for the HS corona (Figure S4, Supporting Information). Although preliminary, these results for silica nanoparticles are in line with many similar reports in literature, where it has been shown that differences in corona composition in FBS and human serum can lead to different uptake by cells.[31,34,46,47] In contrast, in the case of the DOPG-DC liposomes, our results showed that despite the very different coronas formed in the two media, the strong differences in uptake efficiency were mainly due to the different source of the excess free serum proteins in the medium. A possible explanation for this peculiar observation is that the formed corona is not engaging with specific cell receptors or that despite the different corona composition, the two corona-coated liposomes interact with the same receptors via some common component in the two coronas. For instance, mass spectrometry showed that the most abundant protein in the FBS corona was apolipoprotein C-III (around 20% of the total corona proteins), while the most abundant protein in the HS corona was apolipoprotein C-I (also around 20%, see Table S3, Supporting Information). However, both of these apolipoproteins can

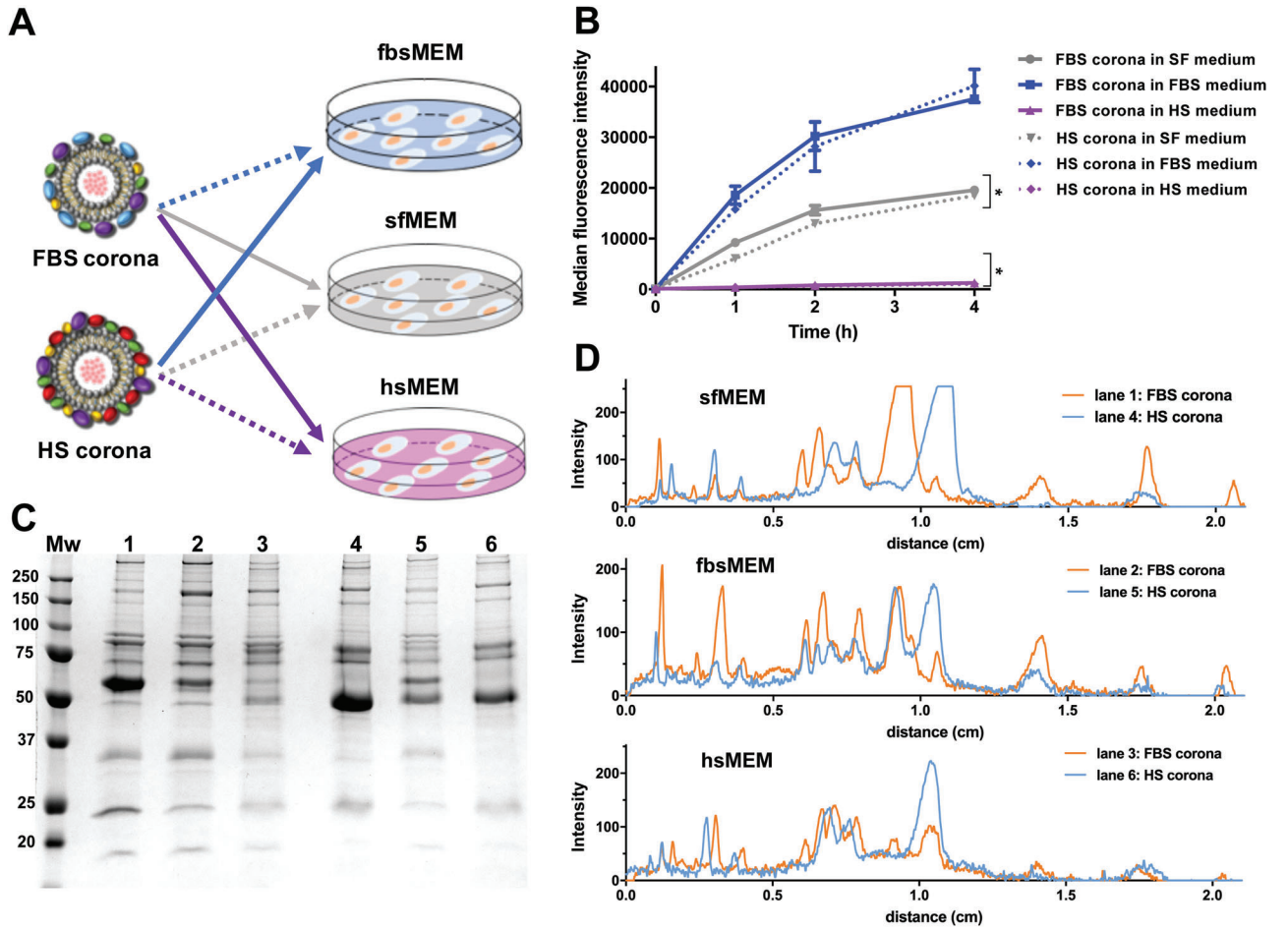

Figure 4. A) Scheme illustrating FBS and HS corona-coated liposomes exposed to cells in sfMEM, fbsMEM, and hsMEM. B) Uptake kinetics of FBS and HS corona-coated liposomes by HeLa cells in different media. FBS corona and HS corona were prepared after incubation of DOPG-DC liposomes with FBS or cleaned HS for 1 h and isolation from excess serum proteins by SEC, as described in the Experimental Section. Then, HeLa cells were exposed to corona-coated liposomes to a final lipid concentration of 50 μg mL^{-1} in serum free medium (sfMEM) and medium supplemented with 4 mg mL^{-1} FBS or HS (fbsMEM and hsMEM) and cell fluorescence measured by flow cytometry. Two independent experiments were conducted with two different batches of liposomes and corona isolations and in each experiment two samples were measured in each condition for each exposure time. The data are the average and standard deviation over duplicate samples of the median cell fluorescence intensity of a representative experiment. A Friedman test with time as blocking factor was performed to compare uptake kinetics of the two different coronas when exposed to cells in the same medium. $p < 0.05$ was considered significant (indicated with *). Though in two cases the differences are statistically significant, it is clear that they are not substantial. Overall, the results thus showed that FBS and HS corona-coated liposomes have comparable uptake efficiency when exposed to cells in the same medium. C) SDS-PAGE image of FBS corona (lane 1), FBS corona reintroduced and recovered from fbsMEM (lane 2) or hsMEM (lane 3), HS corona (lane 4) and HS corona reintroduced and recovered from fbsMEM (lane 5) or hsMEM (lane 6). The same amounts of liposomes were loaded in all lanes (0.025 μmol lipid). D) Intensity profiles of all bands in the SDS-PAGE image shown in Figure 5C. SDS-PAGE and the quantification of the band intensities showed that a different corona was formed after the corona-coated liposomes were reintroduced in medium with serum of a different species. However, differences between the original HS and FBS coronas remained still visible, even after introduction into the same medium (lanes 2 and 5 for fbsMEM and 3 and 6 for hsMEM).

interact with scavenger receptor class B type I (SR-BI), thus they may trigger uptake via the same pathway.[48,49]

At the same time, the different outcome observed in the case of the liposomes highlights that when nanoparticles are exposed to the cells in a medium supplemented with serum from different species, not only the protein corona, but also the excess free serum proteins do play an important role in nanoparticle–cell interactions. The free proteins in human serum are likely to have higher affinity for cell receptors on the human HeLa cells than the proteins in bovine serum. Thus, they may compete with nanoparticles for cell receptors, leading to the lower uptake in HS. Additionally, the amounts of competing free proteins in solution may differ in the two sera. For example, mass spectrometry showed that immunoglobulins accounted for 21% of total proteins in HS, while they were barely detected in FBS (≈0%) (Figure S3C, Supporting Information). Thus, the excess free immunoglobulins present in HS may compete for the Fc gamma RIII receptor, which was previously shown to be involved in nanoparticle uptake,[50] while the competition for similar receptors would be much lower in FBS. Similarly, apolipoprotein B in serum can be recognized by the low-density lipoprotein receptor, while apolipoproteins A-I, A-II, and A-IV can bind to the

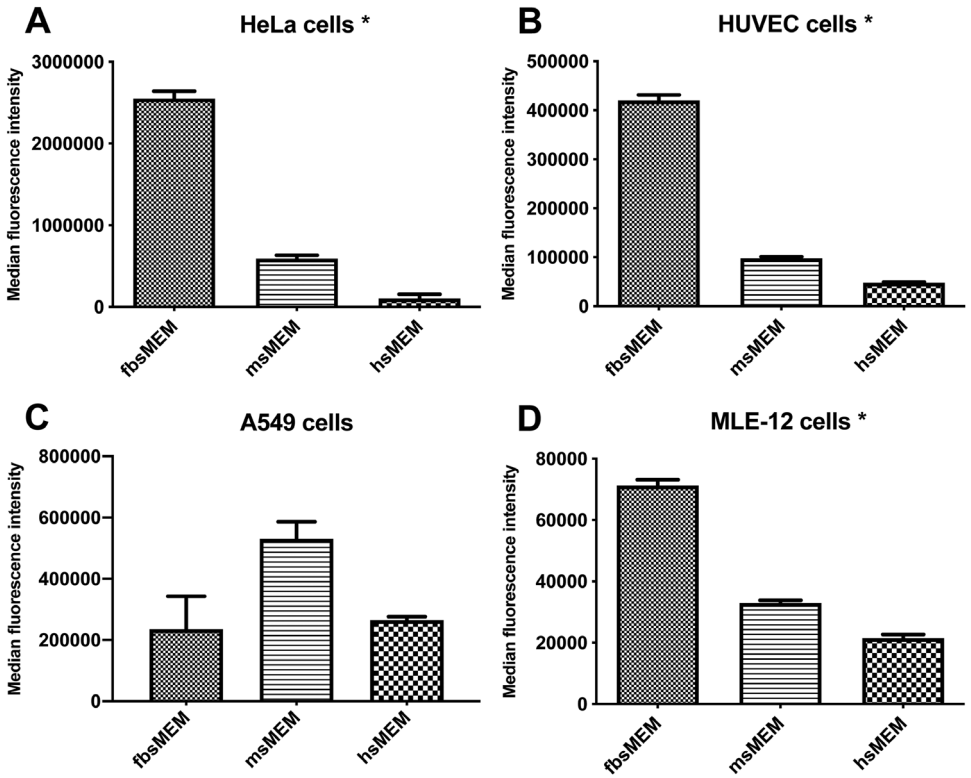

Figure 5. Cellular uptake of DOPG-DC liposomes in different cell lines in medium supplemented with FBS (fbsMEM), mouse serum (msMEM), and human serum (hsMEM). A) Human HeLa, B) HUVEC, and C) A549 cells were exposed for 4 h to 50 μg mL^{-1} DOPG-DC liposomes in medium supplemented with 4 mg mL^{-1} FBS, mouse, or human serum (fbsMEM, msMEM, and hsMEM, respectively). D) Murine MLE-12 cells were exposed for 2 h to 100 μg mL^{-1} DOPG-DC liposomes in the same media. Cells were then collected for flow cytometry measurements. The results are the average and standard deviation over triplicate samples of the median cell fluorescence intensity obtained by flow cytometry in a representative experiment out of 3. For each cell line, a Kruskal–Wallis test was performed to compare uptake levels in the different media. Significant differences were found for the results in HeLa, HUVEC, and MLE-12 cells (panels A, B, and D, respectively). $p < 0.05$ was considered significant (indicated with *).

high-density lipoprotein receptor and SR-BI.[51] Mass spectrometry showed that the total apolipoprotein content was 3% for FBS and 8% for HS. These differences in apolipoprotein content can lead to differences in corona composition, but also to different competition by the free apolipoproteins present in the two sera.

To further test similar effects and, in particular, how liposome uptake varied when the cell and serum species were matched or differed, we performed equivalent experiments in two more human cell lines, namely lung epithelial cancer A549 cells and primary human umbilical vein endothelial cells (HUVEC) together with the HeLa cells, and—in addition—in mouse lung epithelial cells (MLE-12 cells). Then, all the different cell types were exposed to the liposomes in a medium supplemented with 4 mg mL^{-1} human, bovine, as well as mouse serum (hsMEM, fbsMEM, and msMEM, respectively). As shown in **Figure 5**, in HeLa, HUVEC, and MLE-12 cells, uptake was lowest in hsMEM and highest for liposomes in fbsMEM, while in A549 cells uptake was highest in msMEM and comparable in fbsMEM and hsMEM. Overall, these results, although preliminary, confirm that the source of proteins used for exposure to cells strongly affects nanomedicine uptake by cells. When changing the source of proteins used during exposure to cells, not only the corona composition varies, but also the abundance and identity of the free proteins in solution. The free proteins in solution can affect nanomedicine uptake due to competition with cell receptors. Because of this, one may expect a stronger competition when cells and serum species are matched. However, the results of Figure 5 also suggest that this is not always the case, because for the murine cells, the lowest uptake was observed when liposomes were added to cells in human serum and not in mouse serum. A possible explanation is that when changing serum source, the abundance of individual proteins also varies, and it may be that in a different serum, even if from a different species in respect to the cells tested, the concentration of competing proteins is higher than in the serum of the same species, thus leading to lower uptake. Clearly, these effects need to be explicitly tested for every cell, nanomaterial, and biological fluid under study.

3. Conclusions

Biological fluids, such as serum, play an important role in nanoparticle–cell interactions and uptake by cells. On the one hand, proteins and biomolecules can immediately adsorb on the nanoparticle surface forming a corona layer which becomes the real entity that interacts with cells. On the other hand, the excess free proteins in solution also affect uptake by cells since they also interact with cell receptors, thus they may compete with the nanoparticles. In many cases, differences in the corona

forming on nanoparticles when exposed to different types of serum have been shown to lead to differences in uptake,[31,34,46,47] as suggested here for silica nanoparticles (Figure S4, Supporting Information).

However, we also found that in contrast with these observations, in some cases, uptake efficiency may be comparable despite a very different coronas formed on the nanoparticles, as we show here for liposomes in bovine and human serum. This contrasting example allows us to highlight the additional role of the free proteins in solution on nanoparticle outcomes on cells, since in the case of these liposomes, the strong differences in uptake observed in medium supplemented with either bovine or human serum were mainly due to the presence of the excess free proteins in solutions and their species.

Overall, our results confirm that the effects of the serum source on nanoparticle uptake need to be explicitly tested, since when different sera are used not only the corona forming on the nanoparticles will be different (and this can affect in some cases nanoparticle uptake, but not necessarily in all cases), but also the identity and abundance of the free proteins in solution, thus of eventual competing proteins. Additionally, the species of cells used and whether they match or not the serum source introduces further complications in the translation of nanomedicine uptake results across different systems. Thus, when evaluating nanomedicine therapeutic efficiency, using matching serum source (or other relevant biological fluid) and cells, may help to narrow the gap between in vitro and in vivo studies. Similarly, using relevant human cells with human serum or plasma may reduce some of the differences usually observed between preclinical studies and clinical trials. It would be interesting to determine also how similar effects may translate in animal models where diseased human cells or tissues are implanted (for instance xenograft models).[52–54] In such models, the targeted cells/tissues (human) and the serum proteins (of the animal model) are from different species. This may affect uptake efficiency in the targeted cells and contribute, at least in part, to commonly observed differences in nanomedicine efficacy in the translation from animal models to humans. Ultimately, all these factors need to be explicitly tested.

4. Experimental Section

Serum Preparation: FBS (Gibco Thermo Fisher Scientific), human serum (human serum from pooled donors, from TCS Biosciences Ltd) and mouse serum (Envigo) were used for the experiments. Sera were stored at −20 °C and defrosted just before being used.

Preparation and Characterization of Liposomes: DOPG-DC liposomes were prepared by thin lipid film hydration followed by repeated freeze–thaw cycles and extrusion. Briefly, 1,2-dioleoyl-sn-glycero-3-phospho-(1′-rac-glycerol) (DOPG) and 3ß-[*N*-(*N*′,*N*′-dimethylaminoethane)-carbamoyl]cholesterol (DC-cholesterol) (Avanti Polar Lipids) in molar ratio of 2.5: 1 were dissolved in chloroform and the organic solvent was evaporated with a nitrogen stream for 30 min and under vacuum overnight. To label the liposomes with a hydrophilic dye loaded in their aqueous core, the dried lipid films were hydrated with a 25×10^{-3} M solution of sulforhodamine B (SRB) (Thermo Fisher Scientific) in PBS to a final lipid concentration of 10 mg mL^{-1}. To produce unilamellar liposomes, the lipid suspension was frozen into liquid nitrogen and melted in a water bath at 37 °C for 8 freeze–thaw cycles, followed by extrusion for 21 times through a 100 nm polycarbonate membrane using a Avanti Mini-Extruder (Avanti Polar Lipids). To remove the free SRB, the liposome dispersion was then passed through a Zeba Spin Desalting Column, 7K MWCO (molecular weight cut-off) (Thermo Fisher Scientific) pre-equilibrated in PBS. Liposomes were stored in darkness at 4 °C and used for maximum one month after preparation.

The final lipid concentration of the liposomes was quantified based on the Stewart assay.[55] For this, a ferrothiocyanate reagent was prepared with 27.03 mg ferric chloride hexahydrate (Sigma-Aldrich) and 30.4 mg ammonium thiocyanate (Sigma-Aldrich) dissolved in 1 mL Milli-Q water. 10 µL sample was then mixed with 1 mL chloroform and 1 mL ferrothiocyanate reagent followed by vortexing for 60 s and centrifugation at 300 g for 10 min. 0.9 mL of the chloroform phase was transferred to a quartz cuvette and the absorbance at 470 nm measured with a Unicam UV500 Spectrophotometer (Unicam Instruments). Samples of DOPG at known concentration were used to obtain a calibration curve which was used to determine the final lipid concentration of the liposomes.

Size distribution and zeta potential of the DOPG-DC liposomes were measured using a Malvern Zetasizer Nano ZS (Malvern Instruments Ltd). Liposomes were dispersed in different media including PBS, the complete MEM cell culture medium supplemented with 10% FBS, roughly corresponding to 4 mg mL^{-1} serum (fbsMEM) and MEM medium supplemented with 4 mg mL^{-1} human serum (hsMEM). Samples at a final concentration of 50 µg mL^{-1} lipids were prepared by mixing the required volume of the liposome stock solution with the different media and were measured immediately after dispersion. Microcuvettes for 40 µL samples were used for size measurements and disposable folded capillary cells for zeta potential measurements. For each sample three measurements were performed with automatic setting for the measurement duration.

Cell Culture: Human epithelioid cervix carcinoma HeLa cells (from the American Type Culture Collection, ATCC, cell line CCL- -2), adenocarcinomic human alveolar epithelial A549 cells (ATCC cell line CCL-185), primary human umbilical vein endothelial HUVEC from pooled donors (LONZA), and mouse lung epithelial MLE-12 cells (ATCC cell line CRL-2110) were used for in vitro uptake studies. Hela and A549 cells were cultured in fbsMEM in a humidified atmosphere containing 5% CO_2 at 37 °C, passaged two to three times per week and grown for maximum 20 passages after defrosting. HUVEC were cultured in endothelial cell grow medium 2 (ECGM-2) (Bio-Connect) at 5% CO_2 37 °C, and the medium was refreshed every 48 h. To avoid cell senescence and the loss of primary cell characteristics, HUVEC between two and seven passages were used for experiments. MLE-12 cells were cultured in Dulbecco's modified Eagle medium (DMEM) (Gibco) supplemented with 10% FBS, 1% L-glutamine, and 0.01 mg mL^{-1} gentamicine (Gibco) at 5% CO_2 37 °C. MLE-12 cells were passaged every 3–4 d and grown for maximum 20 passages after defrosting. All types of cells were tested for mycoplasma monthly to exclude contamination.

Internalization Studies: Flow cytometry and confocal imaging were used to study the cellular uptake behavior of liposomes in different media. For flow cytometry, in order to study liposome uptake kinetics, HeLa cells were seeded with 5×10^4 cells per well in a 24-well plate and incubated in fbsMEM for 24 h. Before exposure to liposomes, cells were washed three times with serum free medium (sfMEM) and incubated in sfMEM for 30 min. Liposomes were dispersed in fbsMEM or hsMEM at a final concentration of 50 µg mL^{-1} lipids and added to cells immediately after dispersion. Alternatively, to study the uptake behavior of corona-coated liposomes and 100 nm silica nanoparticles (TCS Biosciences) (as a comparison), after isolation of corona-coated liposomes or silica nanoparticles performed as described below, HeLa cells were exposed to 50 µg mL^{-1} corona-coated liposomes or 100 µg mL^{-1} corona-coated silica nanoparticles in either sfMEM, fbsMEM, or hsMEM. Cells were then collected after different incubation times for flow cytometry measurement. Briefly, cells were washed with fbsMEM once and PBS twice to remove excess free nanoparticles and potential nanoparticles adhering outside the cells and harvested by incubation for 5 min with trypsin-ethylenediaminetetraacetic acid (EDTA) (0.05% v/v). The collected cells were then centrifuged at 300 g for 5 min, resuspended in PBS and measured immediately using a BD FACSArray (BD Biosciences) with a 532 nm laser. For cellular uptake of corona-coated silica nanoparticles, cell fluorescence was measured using a Cytoflex S Flow Cytometer (Beckman Coulter) with a 488 nm laser. For

each experiment, a total of at least 2×10^4 cells were acquired per sample and for each condition 2 or 3 replicate samples were included. Experiments were repeated at least two times to confirm reproducibility. Data were analyzed using Flowjo software (FlowJo, LLC). Double scatter forward and side scattering plots were used to exclude cell debris and cell doublets. The results are reported as the averaged median cell fluorescence intensity and standard deviation over duplicate samples.

In order to determine if the internalization of liposomes was energy-dependent, HeLa cells were treated with sodium azide (Merck) to deplete the cell energy. Briefly, 5×10^4 cells per well were seeded in a 24-well plate and incubated in fbsMEM for 24 h. Then, cells were washed with sfMEM for three times and incubated with 5 mg mL^{-1} sodium azide in fbsMEM or hsMEM for 30 min to deplete cell energy. Cells were exposed to 50 µg mL^{-1} liposome dispersions prepared by mixing the liposome stock with fbsMEM or hsMEM in standard conditions or in the presence of 5 mg mL^{-1} sodium azide. Cells were collected at 1, 2, and 3 h after exposure for flow cytometry analysis as described above.

In addition, to compare liposome uptake behavior in different cell lines and in different sera, HeLa and A549 cells were seeded in fbsMEM or MLE-12 cells in complete DMEM with 5×10^4 cells per well in a 24-well plate. For HUVEC cells, wells were precoated with 0.1 mg mL^{-1} cold rat-tail collagen type-I (Corning) for 1 h and washed three times with PBS, then cells were seed at a density of 5×10^4 cell per well in ECGM-2. After 24 h incubation, cells were washed with 1 mL sfMEM. Then HeLa cells, A549 cells, and HUVEC cells were exposed for 4 h to 50 µg mL^{-1} liposomes and MLE-12 for 2 h to 100 µg mL^{-1} liposomes in their respective medium supplemented with 4 mg mL^{-1} FBS (fbsMEM), mouse serum (msMEM), or human serum (hsMEM). Cells were collected as described above for flow cytometry and cell fluorescence measured using a Cytoflex S Flow Cytometer.

Confocal microscopy was used to visualize the cellular uptake of the liposomes in different media. Cells were seeded at a density of 1.5×10^6 cells per well in a 35 mm dish with glass bottom (170 µm thickness). 24 h after seeding, cells were washed three times with sfMEM and incubated in sfMEM for 30 min. A 50 µg mL^{-1} liposome dispersion was prepared by mixing the liposome stock with fbsMEM or hsMEM and incubated with cells for 2 h at 37 °C followed by three washes with sfMEM to remove excess liposome outside cells. To visualize the lysosomes, cells were stained with 100×10^{-9} M LysoTracker Deep Red (Thermo Fisher Scientific) in fbsMEM for 30 min followed by three washes with sfMEM. Finally, cell nuclei were stained by incubation for 5 min with 1 µg mL^{-1} Hoechst 33342 Solution (Thermo Fisher Scientific) in fbsMEM and washed with PBS once. A Leica TCS SP8 confocal fluorescence microscope (Leica Microsystems) was used for cell imaging with a 405 nm laser for Hoechst excitation, a 552 nm laser for liposomes, and a 640 nm laser for LysoTracker Deep Red. For liposome uptake in fbsMEM, images of a representative optical slice were taken every 20 s for up to 3 min and for liposome uptake in hsMEM every 13 s for a total of 2 min. ImageJ software (http://www.fiji.sc) was used for image processing.

Preparation of Corona-Coated Nanoparticles: To isolate corona-coated liposomes from FBS medium, 0.5 mg mL^{-1} DOPG-DC liposomes was mixed with 40 mg mL^{-1} FBS (this corresponds to a final lipid to protein ratio of 1:80 w/w as for the experiments with cells). The sample was incubated in a Thermo-Shaker (Grant Instruments Ltd.) at 37 °C, 250 rpm for 1 h. SEC was then applied to separate liposomes from the excess serum proteins. Briefly, a Sepharose CL-4B (Sigma-Aldrich) column (15 × 1.5 cm) was prepared and equilibrated with PBS. 1 mL of the liposomes in FBS was loaded on the column and the eluent collected immediately. Every 0.5 mL eluent was collected as fraction up to a total volume of 15 mL and the absorption of each fraction was measured at 280 and 565 nm using a NanoDrop One Microvolume UV–vis Spectrophotometer (Thermo Fisher Scientific) in order to determine—respectively—the protein elution profile and the fractions containing the SRB labeled corona-coated liposomes. The fractions containing liposomes were pooled together and a Vivaspin 6 centrifugal concentrator (10 K MWCO, Sartorius) was used to concentrate the sample until less than 200 µL volume was obtained.

To obtain corona-coated liposomes in human serum, first the human serum was depleted of larger objects and protein aggregates of sizes around 100 nm as previously described (The presence of these objects eluting in the same fractions as the corona-coated liposomes could confuse corona identification).[39] Briefly, 1 mL full human serum was loaded on a Sepharose CL-4B column pre-balanced with PBS, and fractions of 0.5 mL were collected until the volume of eluent reached 15 mL. The absorption of each fraction at 280 nm was measured in order to determine the protein elution profile. The fractions from 11 to 30 were pooled together and used as cleaned human serum (cleaned HS). Then, 75 µg mL^{-1} DOPG-DC liposomes was dispersed in 6 mg mL^{-1} cleaned HS (thus maintaining the lipid to protein ratio of 1: 80 w/w as for all other measurements) and incubated on a Thermo-Shaker at 37 °C, 250 rpm for 1 h, followed by corona isolation and concentration as described above.

In order to obtain corona-coated silica nanoparticles, 1 mg mL^{-1} 100 nm green labeled plain silica nanoparticles (Sicastar, Micromod Partikeltechnologie GmbH) were mixed with 40 mg mL^{-1} FBS or human serum and incubated in a Thermo-Shaker at 37 °C, 250 rpm for 1 h. The sample was then centrifuged at 16 000 g 15 °C for 1 h and the pellet containing corona-coated silica nanoparticles was resuspended in 200 µL PBS. In order to determine the concentration of the recovered corona-coated silica nanoparticles, a calibration curve was made using silica nanoparticles in PBS at different concentrations from 0 to 1000 µg mL^{-1} as standards. The fluorescence intensity of corona samples and standards was measured and the concentration was calculated using the standard curve.

Characterization of Corona-Coated Liposomes: After corona isolation, the size distribution of the corona-coated liposomes was measured immediately using a Malvern Zetasizer Nano model ZS as described above. Cryo-EM was used to further confirm the morphology and dispersibility of corona-coated liposomes. Briefly, a few microliter of bare liposomes and corona-coated liposomes isolated from FBS or human serum were deposited separately on a holey carbon coated copper grid (Quantifoil 3.5/1, Quantifoil Micro Tools). After blotting the excess liquid using a Vitrobot mark (Field Electron and Ion Company, FEI), the grids were vitrified in liquid ethane and transferred to a FEI Tecnai T20 cryo-electron microscope equipped with a Gatan model 626 cryo-stage operating at 200k eV. Images were then recorded under low-dose conditions using a low-scan charge-coupled device (CCD) camera.

To compare serum protein binding capacity to liposomes in the different sera, the protein/lipid ratio (µg of protein/µmol of lipid) of corona-coated liposomes recovered from FBS and HS was calculated. The lipid amount in the corona-coated liposomes was quantified with the Stewart assay as described above and the amount of proteins in the corona was determined by Bio-Rad *DC* protein assay (Bio-Rad Laboratories, Inc.). Briefly, dilutions of bovine serum albumin (BSA) from 0.1 to 3.2 mg mL^{-1} were prepared, and 5 µL corona samples and BSA standards were then mixed with the Bio-Rad working reagent separately. The absorbance of each sample at 650 nm was measured after 15 min incubation using a ThermoMAX microplate reader (Molecular Devices, LLC). The protein concentration was calculated according to the standard curve obtained for the BSA standards. In order to exclude potential effects of liposome background on the protein assay, 100 µL PBS and 370 µg mL^{-1} DOPG liposomes were pipetted in an UV star 96-wells plate (Greiner BioOne) and their absorbance from 230 to 900 nm was detected using a Synergy H1 Hybrid Multi-Mode Reader (BioTek Instruments). In addition, a series of BSA solutions with concentration from 0 to 1 mg mL^{-1} was prepared and mixed with PBS or 0.77 mg mL^{-1} DOPG-DC liposomes. The concentration of each sample was determined using the Bio-Rad *DC* protein assay as mentioned above and the standard curves of BSA solutions containing liposomes or only PBS were plotted separately.

1D SDS-PAGE was performed to separate the corona proteins absorbed on the liposome surface. Briefly, corona-coated liposomes corresponding to 40 µg lipid were mixed with 4 × loading buffer to a final volume of 40 µL and boiled for 5 min at 95 °C. 20 µg FBS and human serum proteins were also loaded as controls using the same procedure. Samples were then loaded on a 10% polyacrylamide gel. The gel was run under 120 V for 1 h at room temperature, stained with 0.1% Coomassie blue R-250 in water–methanol–glacial acetic acid (5:4:1) solution with gentle agitation for 30 min, and destained with hot distilled water until the background disappeared. Images were captured by using a ChemiDoc model XRS (Bio-Rad) or a scanning machine. In order to compare the proteins recovered

on different corona-coated liposome samples, the intensity profiles of all bands in the SDS-PAGE image were extracted using Image J (Fiji).

Mass Spectrometry: Corona protein digestion was performed as described by Capriotti et al.[56] Briefly, corona-coated liposomes containing 10 µg proteins were suspended in 40 µL of 8 M urea in 50 × 10^{-3} M NH_4HCO_3 (Sigmal-Aldrich). The protein solution was reduced with 2 µL 200 × 10^{-3} M 1,4-dithiothreitol (DTT) (Sigmal-Aldrich) for 30 min, alkylated with 8 µL 200 × 10^{-3} M iodoacetamide (Sigmal-Aldrich) for 30 min, and incubated with 8 µL 200 × 10^{-3} M DTT again at 56 °C for 30 min. The sample solution was then diluted with 50 × 10^{-3} M NH_4HCO_3 to reach a final urea concentration of 1 M and digested with 2 µg trypsin (Promega Corporation) at 37 °C overnight. Additionally, 10 µg bovine and human serum proteins were digested in the same way as controls.

Digested samples were dried in an Eppendorf centrifugal vacuum concentrator (Sigma-Aldrich) and 0.1% trifluoroacetic acid (TFA) v/v was added to stop the enzymatic reaction. A C18 ZipTip (Merck Millipore Ltd.) was then used to desalt and remove free lipids from the digested samples. Briefly, tips ware washed with acetonitrile (ACN) three times, balanced with 0.1% TFA, loaded with samples, and washed with 0.1% TFA. Finally, the digested peptides binding on the tips were eluted out with 100 µL of 0.1% TFA/50% ACN (50:50, v/v), and the solvent was evaporated using a vacuum centrifuge. The dried peptides were dissolved in 10 µL of 1% HCOOH v/v for LC/MS analysis.

LC-MS/MS was performed using an UltiMate 3000 RSLC ultra high performance liquid chromatography system (Dionex, CA), which was coupled to an Orbitrap Q Exactive Plus mass spectrometer (Thermo Fisher Scientific) with a data-dependent acquisition mode. Peptides (corresponding to 3 µg proteins) were enriched onto an 300 µm i.d. × 5 mm Acclaim PepMap100 C18 trap column (Dionex, #160454) with 5 µm resin size and 100 Å pore size with 0.1% formic acid (FA) at a flow rate of 20 µL min^{-1}, and then separated on an Acclaim PepMap RSLC C18 analytical column (Dionex, #164540; 75 µm i.d. × 500 mm, 2 µm, 100 Å) using a linear 90 min gradient from 3% to 50% eluent B (ACN containing 0.1% FA) in eluent A (H_2O containing 0.1% FA) at 40 °C with a flow rate of 300 nL min^{-1}. During the sample injection interval, the column ran a gradient from 50% to 80% of eluent B in 1 min, then it was kept at 80% eluent B for 9 min, and back to 3% eluent B in 1 min and then equilibrated for 29 min.

Proteomics data were processed using PEAKS Studio 8.5 (Bioinformatics Solutions Inc.) against the SwissProt human database (downloaded on July 27th 2016) or SwissProt bovine database (downloaded on September 24th 2019). Trypsin was selected as proteinase (≤ 2 missed cleavages). Fixed modification was set for carbamidomethylation and variable modification for methionine oxidation and acetylation of protein N-terminal with up to three variable modifications per peptide. In addition, 0.02 Da fragment mass tolerance, 10.0 ppm precursor mass tolerance, and ≤0.1% false discovery rates for peptide-spectrum matches (PSMs) were used. Semi-quantitative evaluation of the protein amount was performed by determining the ion peak intensity (Area), which was the sum of all peptides areas that belong to the same protein group uniquely identified with data-dependent acquisition mode. For each identified protein, the Area was normalized by the protein molecular weight and expressed as the relative protein quantity by applying the following equation

$$\text{Area}_x = \frac{(\text{Area}/M_w)_x}{\sum_{i=1}^{n}(\text{Area}/M_w)_i} \times 100 \quad (1)$$

Identified proteins in each sample were then classified according to their molecular weight and isoelectric point from Proteome Isoelectric Point Database (http://isoelectricpointdb.org/index.html), and functional annotations from Uniprot Database (https://www.uniprot.org/). The relative protein quantity of all proteins belonging to the same classified group was calculated and presented in a stacked column chart. The top 20 most abundant proteins in each sample were ranked according to the calculation in Equation (1).

Statistical Analysis: For DLS and zeta potential measurements, the results are the average and standard deviation over three replicate measurements. For DLS, to allow easier comparison, the size distributions of a representative measurement of each sample are shown after normalization. For flow cytometry, the data were analyzed using Flowjo software (FlowJo, LLC) and the results are the average and standard deviation of the median value of the cell fluorescence distribution obtained by measuring at least 2×10^4 individual cells. For each condition, two or three replicate samples were measured and each experiment was repeated two or three times to confirm reproducibility (as specified in each figure caption).

Statistical differences between two groups were assessed using the nonparametric Mann–Whitney test (two-tailed). For the comparison of multiple groups, Kruskal–Wallis was used. Statistical analysis was performed using GraphPad Prism 9. To assess statistical differences between uptake kinetics in different conditions (Figures 2A–C and 4B), an extension of the nonparametric rank-based Friedman test to multiple observations per cell was used,[57] with time as a blocking factor and replicate samples as multiple observations. A significance level of 5% was used.

Supporting Information

Supporting Information is available from the Wiley Online Library or from the author.

Acknowledgements

K.Y. was supported by a Ph.D. scholarship from the China Scholarship Council. This work was partially supported by the European Research Council (ERC) grant NanoPaths to A.S. (Grant Agreement N 637614). A.S. kindly acknowledges the University of Groningen for additional funding (Rosalind Franklin Fellowship). The authors would like to thank Robbert Hans Cool (University of Groningen) for technical help and suggestions for size exclusion chromatography. Mass spectrometry analysis was performed in the Interfaculty Mass Spectrometry Center of the University of Groningen and University Medical Center Groningen (UMCG). The authors would like to thank H. Permentier and C.M. Jeronimus-Stratingh for technical help and suggestions for sample preparation for mass spectrometry. Prof. Ingrid Molema (UMCG) is kindly acknowledged for supplying the mouse MLE-12 cells and Barbara Mesquita for technical help with preliminary studies. Christoffer Åberg (University of Groningen) is acknowledged for assistance with statistical analysis.

Conflict of Interest

The authors declare no conflict of interest.

Data Availability Statement

The data that support the findings of this study are available from the corresponding author upon reasonable request.

Keywords

liposome–cell interactions, liposomes, protein corona, protein sources

Received: February 26, 2021
Revised: April 19, 2021
Published online: May 29, 2021

[1] B. Pelaz, C. Alexiou, R. A. Alvarez-Puebla, F. Alves, A. M. Andrews, S. Ashraf, L. P. Balogh, L. Ballerini, A. Bestetti, C. Brendel, S. Bosi, M. Carril, W. C. W. Chan, C. Chen, X. Chen, X. Chen, Z. Cheng, D. Cui, J. Du, C. Dullin, A. Escudero, N. Feliu, M. Gao, M. George, Y. Gogotsi, A. Gru, Z. Gu, N. J. Halas, N. Hampp, R. K. Hartmann, et al., *ACS Nano* **2017**, *11*, 2313.

[2] M. Ferrari, *Nat. Rev. Cancer* **2005**, *5*, 161.
[3] D. Peer, J. M. Karp, S. Hong, O. C. Farokhzad, R. Margalit, R. Langer, *Nat. Nanotechnol.* **2007**, *2*, 751.
[4] L. Zhang, F. Gu, J. Chan, A. Wang, R. Langer, O. Farokhzad, *Clin. Pharmacol. Ther.* **2008**, *83*, 761.
[5] Y. Noguchi, J. Wu, R. Duncan, J. Strohalm, K. Ulbrich, T. Akaike, H. Maeda, *Jpn. J. Cancer Res.* **1998**, *89*, 307.
[6] A. K. Iyer, G. Khaled, J. Fang, H. Maeda, *Drug Discovery Today* **2006**, *11*, 812.
[7] K. Greish, H. Nehoff, N. Parayath, L. Domanovitch, S. Taurin, *Int. J. Nanomed.* **2014**, *9*, 2539.
[8] V. Wagner, A. Dullaart, A.-K. Bock, A. Zweck, *Nat. Biotechnol.* **2006**, *24*, 1211.
[9] M. E. Davis, Z. Chen, D. M. Shin, *Nat. Rev. Drug Discovery* **2008**, *7*, 771.
[10] F. Danhier, O. Feron, V. Préat, *J. Controlled Release* **2010**, *148*, 135.
[11] K. Park, *J. Controlled Release* **2017**, *267*, 2.
[12] S. Hua, M. B. C. de Matos, J. M. Metselaar, G. Storm, *Front. Pharmacol.* **2018**, *9*, 790.
[13] J. I. Hare, T. Lammers, M. B. Ashford, S. Puri, G. Storm, S. T. Barry, *Adv. Drug Delivery Rev.* **2017**, *108*, 25.
[14] G. Gstraunthaler, T. Lindl, J. van der Valk, *Cytotechnology* **2013**, *65*, 791.
[15] T. Cedervall, I. Lynch, S. Lindman, T. Berggård, E. Thulin, H. Nilsson, K. A. Dawson, S. Linse, T. Berggard, E. Thulin, H. Nilsson, K. A. Dawson, S. Linse, *Proc. Natl. Acad. Sci. U. S. A.* **2007**, *104*, 2050.
[16] A. E. Nel, L. Mädler, D. Velegol, T. Xia, E. M. V. Hoek, P. Somasundaran, F. Klaessig, V. Castranova, M. Thompson, *Nat. Mater.* **2009**, *8*, 543.
[17] C. D. Walkey, W. C. W. Chan, *Chem. Soc. Rev.* **2012**, *41*, 2780.
[18] M. P. Monopoli, C. Åberg, A. Salvati, K. A. Dawson, *Nat. Nanotechnol.* **2012**, *7*, 779.
[19] A. Salvati, A. S. Pitek, M. P. Monopoli, K. Prapainop, F. B. Bombelli, D. R. Hristov, P. M. Kelly, C. Åberg, E. Mahon, K. A. Dawson, *Nat. Nanotechnol.* **2013**, *8*, 137.
[20] S. Tenzer, D. Docter, J. Kuharev, A. Musyanovych, V. Fetz, R. Hecht, F. Schlenk, D. Fischer, K. Kiouptsi, C. Reinhardt, K. Landfester, H. Schild, M. Maskos, S. K. Knauer, R. H. Stauber, *Nat. Nanotechnol.* **2013**, *8*, 772.
[21] J. Lazarovits, S. Sindhwani, A. J. Tavares, Y. Zhang, F. Song, J. Audet, J. R. Krieger, A. M. Syed, B. Stordy, W. C. W. Chan, *ACS Nano* **2019**, *13*, 8023.
[22] Z. J. Deng, M. Liang, M. Monteiro, I. Toth, R. F. Minchin, *Nat. Nanotechnol.* **2011**, *6*, 39.
[23] S. Lara, F. Alnasser, E. Polo, D. Garry, M. C. Lo Giudice, D. R. Hristov, L. Rocks, A. Salvati, Y. Yan, K. A. Dawson, *ACS Nano* **2017**, *11*, 1884.
[24] G. Caracciolo, F. Cardarelli, D. Pozzi, F. Salomone, G. Maccari, G. Bardi, A. L. Capriotti, C. Cavaliere, M. Papi, A. Laganà, *ACS Appl. Mater. Interfaces* **2013**, *5*, 13171.
[25] A. Lesniak, F. Fenaroli, M. P. Monopoli, C. Åberg, K. A. Dawson, A. Salvati, *ACS Nano* **2012**, *6*, 5845.
[26] D. Chen, N. Parayath, S. Ganesh, W. Wang, M. Amiji, *Nanoscale* **2019**, *11*, 18806.
[27] G. Maiorano, S. Sabella, B. Sorce, V. Brunetti, M. A. Malvindi, R. Cingolani, P. P. Pompa, *ACS Nano* **2010**, *4*, 7481.
[28] M. Bros, L. Nuhn, J. Simon, L. Moll, V. Mailänder, K. Landfester, S. Grabbe, *Front. Immunol.* **2018**, *9*, 1760.
[29] A. Solorio-Rodríguez, V. Escamilla-Rivera, M. Uribe-Ramírez, A. Chagolla, R. Winkler, C. M. García-Cuellar, A. De Vizcaya-Ruiz, *Nanoscale* **2017**, *9*, 13651.
[30] L. K. Müller, J. Simon, C. Rosenauer, V. Mailänder, S. Morsbach, K. Landfester, *Biomacromolecules* **2018**, *19*, 374.
[31] S. Schöttler, K. Klein, K. Landfester, V. Mailänder, *Nanoscale* **2016**, *8*, 5526.
[32] S. Laurent, C. Burtea, C. Thirifays, F. Rezaee, M. Mahmoudi, *J. Colloid Interface Sci.* **2013**, *392*, 431.
[33] H. Mohammad-Beigi, C. Scavenius, P. B. Jensen, K. Kjaer-Sorensen, C. Oxvig, T. Boesen, J. J. Enghild, D. S. Sutherland, Y. Hayashi, *ACS Nano* **2020**, *14*, 10666.
[34] C. Pisani, E. Rascol, C. Dorandeu, J.-C. Gaillard, C. Charnay, Y. Guari, J. Chopineau, J. Armengaud, J.-M. Devoisselle, O. Prat, *PLoS One* **2017**, *12*, e0182906.
[35] J. A. Kim, A. Salvati, C. Åberg, K. A. Dawson, *Nanoscale* **2014**, *6*, 14180.
[36] T. M. Allen, P. R. Cullis, *Adv. Drug Delivery Rev.* **2013**, *65*, 36.
[37] U. Bulbake, S. Doppalapudi, N. Kommineni, W. Khan, *Pharmaceutics* **2017**, *9*, 12.
[38] K. Sou, Y. Naito, T. Endo, S. Takeoka, E. Tsuchida, *Biotechnol. Prog.* **2003**, *19*, 1547.
[39] K. Yang, B. Mesquita, P. Horvatovich, A. Salvati, *Acta Biomater.* **2020**, *106*, 314.
[40] G. Caracciolo, D. Pozzi, A. L. Capriotti, C. Cavaliere, S. Piovesana, G. La Barbera, A. Amici, A. Laganà, *J. Mater. Chem. B* **2014**, *2*, 7419.
[41] M. Hadjidemetriou, Z. Al-Ahmady, M. Mazza, R. F. Collins, K. Dawson, K. Kostarelos, *ACS Nano* **2015**, *9*, 8142.
[42] A. L. Capriotti, G. Caracciolo, C. Cavaliere, V. Colapicchioni, S. Piovesana, D. Pozzi, A. Laganà, *Chromatographia* **2014**, *77*, 755.
[43] M. P. Monopoli, D. Walczyk, A. Campbell, G. Elia, I. Lynch, F. Baldelli Bombelli, K. A. Dawson, *J. Am. Chem. Soc.* **2011**, *133*, 2525.
[44] M.-P. Caby, D. Lankar, C. Vincendeau-Scherrer, G. Raposo, C. Bonnerot, *Int. Immunol.* **2005**, *17*, 879.
[45] K. Kristensen, T. B. Engel, A. Stensballe, J. B. Simonsen, T. L. Andresen, *J. Controlled Release* **2019**, *307*, 1.
[46] K. Partikel, R. Korte, D. Mulac, H.-U. Humpf, K. Langer, *Beilstein J. Nanotechnol.* **2019**, *10*, 1002.
[47] V. Francia, K. Yang, S. Deville, C. Reker-Smit, I. Nelissen, A. Salvati, *ACS Nano* **2019**, *13*, 11107.
[48] E. V. Fuior, A. V. Gafencu, *Int. J. Mol. Sci.* **2019**, *20*, 5939.
[49] M. Luo, D. Peng, *Lipids Health Dis.* **2016**, *15*, 184.
[50] H. Su, G. J. Spangrude, H. D. Caldwell, *Infect. Immun.* **1991**, *59*, 3811.
[51] A. Blanco, G. Blanco, in *Medical Biochemistry*, Academic Press, Cambridge, Massachusetts **2017**, pp. 325–365.
[52] X. Xue, Y. Huang, R. Bo, B. Jia, H. Wu, Y. Yuan, Z. Wang, Z. Ma, D. Jing, X. Xu, W. Yu, T. Lin, Y. Li, *Nat. Commun.* **2018**, *9*, 3653.
[53] W. Han, L. Shi, L. Ren, L. Zhou, T. Li, Y. Qiao, H. Wang, *Signal Transduction Targeted Ther.* **2018**, *3*, 16.
[54] J. Lang, X. Zhao, X. Wang, Y. Zhao, Y. Li, R. Zhao, K. Cheng, Y. Li, X. Han, X. Zheng, H. Qin, M. Geranpayehvaghei, J. Shi, G. J. Anderson, J. Hao, H. Ren, G. Nie, *ACS Nano* **2019**, *26*, 2176.
[55] J. C. M. Stewart, *Anal. Biochem.* **1980**, *104*, 10.
[56] A. L. Capriotti, G. Caracciolo, C. Cavaliere, C. Crescenzi, D. Pozzi, A. Laganà, *Anal. Bioanal. Chem.* **2011**, *401*, 1195.
[57] W. J. Conover, in *Practical Nonparametric Statistics*, John Wiley and Sons, New York **1999**, pp. 269–427.